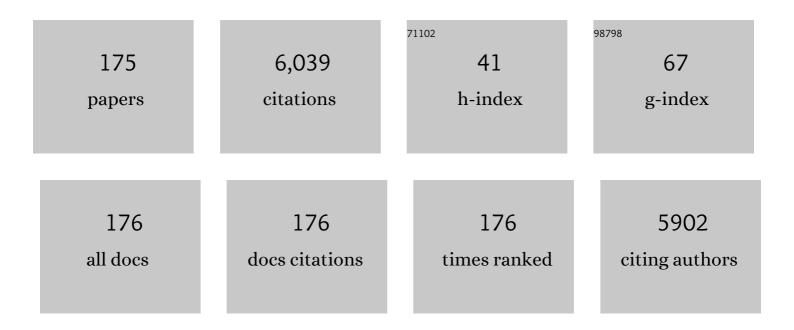
Liang Zhang

List of Publications by Year in descending order

Source: https://exaly.com/author-pdf/423796/publications.pdf Version: 2024-02-01



μανό Ζηλνό

#	Article	IF	CITATIONS
1	Two-sample Behrens–Fisher problems for high-dimensional data: a normal reference scale-invariant test. Journal of Applied Statistics, 2023, 50, 456-476.	1.3	2
2	Wave propagation characteristics and absorbed energy capability of the electrically doubly curved system reinforced by nanocomposite on viscoelastic substrate. Mechanics Based Design of Structures and Machines, 2023, 51, 2794-2811.	4.7	1
3	Multi-system fusion based on deep neural network and cloud edge computing and its application in in in intelligent manufacturing. Neural Computing and Applications, 2022, 34, 3411-3420.	5.6	15
4	Global Incidence, Progression, and Risk Factors of Age-Related Macular Degeneration and Projection of Disease Statistics in 30 Years: A Modeling Study. Gerontology, 2022, 68, 721-735.	2.8	20
5	Stabilized Long-Distance Superluminal Propagation Based on Polarization-Matched Low-Noise Brillouin Lasing Resonance. IEEE Photonics Journal, 2022, 14, 1-6.	2.0	2
6	Effect of sludge retention time on microbial succession and assembly in thermal hydrolysis pretreated sludge digesters: Deterministic versus stochastic processes. Water Research, 2022, 209, 117900.	11.3	30
7	Frequency-stabilized Brillouin random fiber laser enabled by self-inscribed transient population grating. Optics Letters, 2022, 47, 150.	3.3	13
8	Metallogenic â€~factories' and resultant highly anomalous mineral endowment on the craton margins of China. Geoscience Frontiers, 2022, 13, 101339.	8.4	9
9	NOB suppression strategies in a mainstream membrane aerated biofilm reactor under exceptionally low lumen pressure. Chemosphere, 2022, 290, 133386.	8.2	16
10	UAV-Assisted Edge Computing and Streaming for Wireless Virtual Reality: Analysis, Algorithm Design, and Performance Guarantees. IEEE Transactions on Vehicular Technology, 2022, 71, 3267-3275.	6.3	20
11	Quasi-Distributed Magnetic Field Fiber Sensors Integrated with Magnetostrictive Rod in OFDR System. Electronics (Switzerland), 2022, 11, 1013.	3.1	4
12	Using Mechanically-Induced Long-Period Fiber Gratings for OAM Modes Generation Based on Anti-Resonant Mechanisms in Ring-Core Fibers. IEEE Photonics Journal, 2022, 14, 1-6.	2.0	0
13	Responses of mesophilic anaerobic sludge microbiota to thermophilic conditions: Implications for start-up and operation of thermophilic THP-AD systems. Water Research, 2022, 216, 118332.	11.3	17
14	Metagenomic assembled genomes unravel purple non‑sulfur bacteria (PNSB) involved in integrating C, N, P biotransformation. Science of the Total Environment, 2022, 830, 154591.	8.0	4
15	Fabrication and Characterization of Low-Loss Gaussian-Like Reversed Ridge Optical Waveguides. IEEE Photonics Technology Letters, 2022, 34, 649-652.	2.5	3
16	Study on the Hydrogen Embrittlement of Nanograined Materials with Different Grain Sizes by Atomistic Simulation. Materials, 2022, 15, 4589.	2.9	1
17	Genome-centric metagenomics analysis revealed the metabolic function of abundant microbial communities in thermal hydrolysis-assisted thermophilic anaerobic digesters under propionate stress. Bioresource Technology, 2022, 360, 127574.	9.6	12
18	Interaction of perfluorooctanoic acid with extracellular polymeric substances - Role of protein. Journal of Hazardous Materials, 2021, 401, 123381.	12.4	49

#	Article	IF	CITATIONS
19	Top-N recommendation algorithm integrated neural network. Neural Computing and Applications, 2021, 33, 3881-3889.	5.6	5
20	Referral for disease-related visual impairment using retinal photograph-based deep learning: a proof-of-concept, model development study. The Lancet Digital Health, 2021, 3, e29-e40.	12.3	20
21	Dynamic vortex mode-switchable erbium-doped Brillouin laser pumped by high-order mode. Optics Letters, 2021, 46, 468.	3.3	10
22	Underwater acoustic source localization based on phase-sensitive optical time domain reflectometry. Optics Express, 2021, 29, 12880.	3.4	15
23	Pathways and Mechanisms of Single-Cell Protein Production: Carbon and Nutrient Transformation. ACS ES&T Water, 2021, 1, 1313-1320.	4.6	1
24	On the vibrations of the non-polynomial viscoelastic composite open-type shell under residual stresses. Composite Structures, 2021, 263, 113599.	5.8	46
25	High-Sensitivity Bending Sensor Based on Supermode Interference in Coupled Four-Core Sapphire-Derived Fiber. Journal of Lightwave Technology, 2021, 39, 3932-3940.	4.6	10
26	Influence of Temperature on All-Silica Fabry-Pérot Pressure Sensor. IEEE Photonics Journal, 2021, 13, 1-9.	2.0	3
27	Review on Fiber-Optic Vortices and Their Sensing Applications. Journal of Lightwave Technology, 2021, 39, 3740-3750.	4.6	25
28	Optimizing the Operation Cost for UAV-Aided Mobile Edge Computing. IEEE Transactions on Vehicular Technology, 2021, 70, 6085-6093.	6.3	40
29	Molecular dynamics simulation and machine learning of mechanical response in non-equiatomic FeCrNiCoMn high-entropy alloy. Journal of Materials Research and Technology, 2021, 13, 2043-2054.	5.8	32
30	Pyrite assisted peroxymonosulfate sludge conditioning: Uncover triclosan transformation during treatment. Journal of Hazardous Materials, 2021, 413, 125368.	12.4	23
31	Compound Fabry–Pérot interferometer for simultaneous high-pressure and high-temperature measurement. Optics Express, 2021, 29, 24289.	3.4	6
32	Subduction: The recycling engine room for global metallogeny. Ore Geology Reviews, 2021, 134, 104130.	2.7	21
33	Cylindrical Vector Beam for Vector Magnetic Field Sensing Based on Magnetic Fluid. IEEE Photonics Technology Letters, 2021, 33, 703-706.	2.5	4
34	Active learning strategy for high fidelity short-term data-driven building energy forecasting. Energy and Buildings, 2021, 244, 111026.	6.7	24
35	Low-velocity impact, resonance, and frequency responses of FG-GPLRC viscoelastic doubly curved panel. Composite Structures, 2021, 269, 114000.	5.8	38
36	Dynamic mode-switchable and wavelength-tunable Brillouin random fiber laser by a high-order mode pump. Optics Express, 2021, 29, 34109.	3.4	4

#	Article	IF	CITATIONS
37	Triclosan transformation and impact on an elemental sulfur-driven sulfidogenic process. Chemical Engineering Journal, 2021, 421, 129634.	12.7	12
38	Metagenomic insights into the effect of thermal hydrolysis pre-treatment on microbial community of an anaerobic digestion system. Science of the Total Environment, 2021, 791, 148096.	8.0	31
39	Data-driven building energy modeling with feature selection and active learning for data predictive control. Energy and Buildings, 2021, 252, 111436.	6.7	20
40	Laser Charging Enabled DBS Placement for Downlink Communications. IEEE Transactions on Network Science and Engineering, 2021, 8, 3009-3018.	6.4	9
41	Understanding the Radiation Resistance Mechanisms of Nanocrystalline Metals from Atomistic Simulation. Metals, 2021, 11, 1875.	2.3	3
42	A holistic model for the origin of orogenic gold deposits and its implications for exploration. Mineralium Deposita, 2020, 55, 275-292.	4.1	223
43	Utilization of pre-existing competent and barren quartz veins as hosts to later orogenic gold ores at Huangjindong gold deposit, Jiangnan Orogen, southern China. Mineralium Deposita, 2020, 55, 363-380.	4.1	36
44	Relative roles of formation and preservation on gold endowment along the Sanshandao gold belt in the Jiaodong gold province, China: importance for province- to district-scale gold exploration. Mineralium Deposita, 2020, 55, 325-344.	4.1	30
45	Flexible backhaul-aware DBS-aided HetNet with IBFD communications. ICT Express, 2020, 6, 48-56.	4.8	7
46	Unveiling the role of activated carbon on hydrolysis process in anaerobic digestion. Bioresource Technology, 2020, 296, 122366.	9.6	28
47	Optimizing the Deployment and Throughput of DBSs for Uplink Communications. IEEE Open Journal of Vehicular Technology, 2020, 1, 18-28.	4.9	8
48	Mechanical response and plastic deformation of coherent twin boundary with perfect and defective structures. Mechanics of Materials, 2020, 141, 103266.	3.2	10
49	Quorum quenching altered microbial diversity and activity of anaerobic membrane bioreactor (AnMBR) and enhanced methane generation. Bioresource Technology, 2020, 315, 123862.	9.6	32
50	Classroom Status Hierarchy Moderates the Association between Social Dominance Goals and Bullying Behavior in Middle Childhood and Early Adolescence. Journal of Youth and Adolescence, 2020, 49, 2285-2297.	3.5	23
51	Biological conversion of sulfamethoxazole in an autotrophic denitrification system. Water Research, 2020, 185, 116156.	11.3	50
52	Elemental sulfur-driven sulfidogenic process under highly acidic conditions for sulfate-rich acid mine drainage treatment: Performance and microbial community analysis. Water Research, 2020, 185, 116230.	11.3	25
53	Image Recommendation Algorithm Based on Deep Learning. IEEE Access, 2020, 8, 132799-132807.	4.2	15
54	A Simple Scale-Invariant Two-Sample Test for High-dimensional Data. Econometrics and Statistics, 2020, 14, 131-144.	0.8	5

#	Article	IF	CITATIONS
55	A Pattern-Recognition-Based Ensemble Data Imputation Framework for Sensors from Building Energy Systems. Sensors, 2020, 20, 5947.	3.8	7
56	Identification of type 2 diabetes loci in 433,540 East Asian individuals. Nature, 2020, 582, 240-245.	27.8	282
57	Mesozoic Orogenic Gold Mineralization in the Jiaodong Peninsula, China: A Focused Event at 120 ± 2 Ma During Cooling of Pregold Granite Intrusions. Economic Geology, 2020, 115, 415-441.	3.8	110
58	Parenting Practices, Family Obligation, and Adolescents' Academic Adjustment: Cohort Differences with Social Change in China. Journal of Research on Adolescence, 2020, 30, 721-734.	3.7	9
59	Parenting Practices and Adolescent Effortful Control: MAOA T941G Gene Polymorphism as a Moderator. Frontiers in Psychology, 2020, 11, 60.	2.1	4
60	Effects of low doses of UV-B radiation supplementation on tuber quality in purple potato (<i>Solanum tuberosum</i> L.). Plant Signaling and Behavior, 2020, 15, 1783490.	2.4	8
61	Latency-Aware IoT Service Provisioning in UAV-Aided Mobile-Edge Computing Networks. IEEE Internet of Things Journal, 2020, 7, 10573-10580.	8.7	93
62	Mechanistic insights into a novel nitrilotriacetic acid-Fe0 and CaO2 process for efficient anaerobic digestion sludge dewatering at near-neutral pH. Water Research, 2020, 184, 116149.	11.3	43
63	Association of Cataract Surgery With Risk of Diabetic Retinopathy Among Asian Participants in the Singapore Epidemiology of Eye Diseases Study. JAMA Network Open, 2020, 3, e208035.	5.9	7
64	Theoretical and Experimental Study on the Transmission Loss of a Side Outlet Muffler. Shock and Vibration, 2020, 2020, 1-8.	0.6	8
65	High-Efficiency Random Fiber Laser Based on Strong Random Fiber Grating for MHz Ultrasonic Sensing. IEEE Sensors Journal, 2020, 20, 5885-5892.	4.7	20
66	3D Printing Technique-Improved Phase-Sensitive OTDR for Breakdown Discharge Detection of Gas-Insulated Switchgear. Sensors, 2020, 20, 1045.	3.8	16
67	ls kidney function associated with primary open-angle glaucoma? Findings from the Asian Eye Epidemiology Consortium. British Journal of Ophthalmology, 2020, 104, bjophthalmol-2019-314890.	3.9	13
68	Developmental changes in associations between depressive symptoms and peer relationships: a four-year follow-up of Chinese adolescents. Journal of Youth and Adolescence, 2020, 49, 1913-1927.	3.5	13
69	Study of deformation behaviors of martensitic steel quenched at ultralow temperature. Materials Science & Engineering A: Structural Materials: Properties, Microstructure and Processing, 2020, 785, 139399.	5.6	2
70	Inverse Hall-Petch relationship of high-entropy alloy by atomistic simulation. Materials Letters, 2020, 274, 128024.	2.6	60
71	Unveiling delay-time-resolved phase noise statistics of narrow-linewidth laser via coherent optical time domain reflectometry. Optics Express, 2020, 28, 6719.	3.4	12
72	Developmental changes in longitudinal associations between academic achievement and psychopathological symptoms from late childhood to middle adolescence. Journal of Child Psychology and Psychiatry and Allied Disciplines, 2019, 60, 178-188.	5.2	55

#	Article	IF	CITATIONS
73	Bidirectional Associations between Peer Relations and Attention Problems from 9 to 16 Years. Journal of Abnormal Child Psychology, 2019, 47, 381-392.	3.5	13
74	Family socioeconomic status and Chinese children's early academic development: Examining child-level mechanisms. Contemporary Educational Psychology, 2019, 59, 101792.	2.9	31
75	Fast-Moving Jamming Suppression for UAV Navigation: A Minimum Dispersion Distortionless Response Beamforming Approach. IEEE Transactions on Vehicular Technology, 2019, 68, 7815-7827.	6.3	20
76	Approximate Algorithms for 3-D Placement of IBFD Enabled Drone-Mounted Base Stations. IEEE Transactions on Vehicular Technology, 2019, 68, 7715-7722.	6.3	16
77	Enhanced removal of pharmaceuticals in a biofilter: Effects of manipulating co-degradation by carbon feeding. Chemosphere, 2019, 236, 124303.	8.2	45
78	Numerical study of scattering Legendre moments and effect of anisotropic scattering on SN shielding calculation. Nuclear Science and Techniques/Hewuli, 2019, 30, 1.	3.4	3
79	Sensing Matrix Design for MMV Compressive Sensing: An MVDR Approach. IEEE Transactions on Vehicular Technology, 2019, 68, 8601-8612.	6.3	5
80	Ab initio calculations for the H-decorated neutral and charged oxygen vacancy in erbium oxide. Fusion Engineering and Design, 2019, 144, 188-192.	1.9	2
81	At the intersection of exocytosis and endocytosis in plants. New Phytologist, 2019, 224, 1479-1489.	7.3	63
82	Removal of sulfamethoxazole (SMX) in sulfate-reducing flocculent and granular sludge systems. Bioresource Technology, 2019, 288, 121592.	9.6	30
83	Interaction between nano-voids and migrating grain boundary by molecular dynamics simulation. Acta Materialia, 2019, 173, 206-224.	7.9	52
84	Dose-dependent effects of acetate on the biodegradation of pharmaceuticals in moving bed biofilm reactors. Water Research, 2019, 159, 302-312.	11.3	52
85	Corrigendum to "Structural geometry of orogenic gold deposits: Implications for exploration of world-class and giant deposits―[Geoscience Frontiers 9, (2018) 1163–1177]. Geoscience Frontiers, 2019, 10, 789.	8.4	0
86	A Framework for 5G Networks with In-Band Full-Duplex Enabled Drone-Mounted Base-Stations. IEEE Wireless Communications, 2019, 26, 121-127.	9.0	33
87	Process and Mechanism of Gold Mineralization at the Zhengchong Gold Deposit, Jiangnan Orogenic Belt: Evidence from the Arsenopyrite and Chlorite Mineral Thermometers. Minerals (Basel,) Tj ETQq1 1 0.784314	rg₽.To/Ov	erlazk 10 Tf 5
88	Systematic evaluation of a dynamic sewer process model for prediction of odor formation and mitigation in large-scale pressurized sewers in Hong Kong. Water Research, 2019, 154, 94-103.	11.3	41
89	Anatomy of a world-class epizonal orogenic-gold system: A holistic thermochronological analysis of the Xincheng gold deposit, Jiaodong Peninsula, eastern China. Gondwana Research, 2019, 70, 50-70.	6.0	32
90	SoarNet. IEEE Wireless Communications, 2019, 26, 37-43.	9.0	25

#	Article	IF	CITATIONS
91	Secretion of Phospholipase DδFunctions as a Regulatory Mechanism in Plant Innate Immunity. Plant Cell, 2019, 31, 3015-3032.	6.6	55
92	On the Number and 3-D Placement of In-Band Full-Duplex Enabled Drone-Mounted Base-Stations. IEEE Wireless Communications Letters, 2019, 8, 221-224.	5.0	26
93	Electroactive biofilm-based constructed wetland (EABB-CW): A mesocosm-scale test of an innovative setup for wastewater treatment. Science of the Total Environment, 2019, 659, 796-806.	8.0	60
94	Grain boundary induced deformation mechanisms in nanocrystalline Al by molecular dynamics simulation: From interatomic potential perspective. Computational Materials Science, 2019, 156, 421-433.	3.0	42
95	Numerical analysis of spatial discretization schemes in ARES transport code for shielding calculation. Progress in Nuclear Energy, 2019, 110, 236-244.	2.9	4
96	Microbial community metabolic profiles in saturated constructed wetlands treating iohexol and ibuprofen. Science of the Total Environment, 2019, 651, 1926-1934.	8.0	23
97	Ultrasound sensing based on an in-fiber dual-cavity Fabry–Perot interferometer. Optics Letters, 2019, 44, 3606.	3.3	42
98	Thermal and acoustic noise insensitive Brillouin random fiber laser based on polarization-maintaining random fiber grating. Optics Letters, 2019, 44, 4195.	3.3	16
99	A novel elemental sulfur reduction and sulfide oxidation integrated process for wastewater treatment and sulfur recycling. Chemical Engineering Journal, 2018, 342, 438-445.	12.7	46
100	Long-Term Feeding of Elemental Sulfur Alters Microbial Community Structure and Eliminates Mercury Methylation Potential in Sulfate-Reducing Bacteria Abundant Activated Sludge. Environmental Science & Technology, 2018, 52, 4746-4753.	10.0	40
101	Energy-Aware Virtual Machine Management in Inter-Datacenter Networks Over Elastic Optical Infrastructure. IEEE Transactions on Green Communications and Networking, 2018, 2, 305-315.	5.5	15
102	Shear response of grain boundaries with metastable structures by molecular dynamics simulations. Modelling and Simulation in Materials Science and Engineering, 2018, 26, 035008.	2.0	19
103	Multi-Wavelength Brillouin Random Fiber Laser via Distributed Feedback From a Random Fiber Grating. Journal of Lightwave Technology, 2018, 36, 2122-2128.	4.6	55
104	Impacts of design configuration and plants on the functionality of the microbial community of mesocosm-scale constructed wetlands treating ibuprofen. Water Research, 2018, 131, 228-238.	11.3	48
105	Realizing high-rate sulfur reduction under sulfate-rich conditions in a biological sulfide production system to treat metal-laden wastewater deficient in organic matter. Water Research, 2018, 131, 239-245.	11.3	71
106	Linearly Polarized Multi-Wavelength Fiber Laser Comb via Brillouin Random Lasing Oscillation. IEEE Photonics Technology Letters, 2018, 30, 1005-1008.	2.5	9
107	Biological Sulfur Reduction To Generate H ₂ S As a Reducing Agent To Achieve Simultaneous Catalytic Removal of SO ₂ and NO and Sulfur Recovery from Flue Gas. Environmental Science & Technology, 2018, 52, 4754-4762.	10.0	26
108	Structural geometry of orogenic gold deposits: Implications for exploration of world-class and giant deposits. Geoscience Frontiers, 2018, 9, 1163-1177.	8.4	160

#	Article	IF	CITATIONS
109	Multiwavelength Coherent Brillouin Random Fiber Laser With Ultrahigh Optical Signal-to-Noise Ratio. IEEE Journal of Selected Topics in Quantum Electronics, 2018, 24, 1-8.	2.9	22
110	Removal of the pesticide tebuconazole in constructed wetlands: Design comparison, influencing factors and modelling. Environmental Pollution, 2018, 233, 71-80.	7.5	62
111	Deformation twinning and dislocation processes in nanotwinned copper by molecular dynamics simulations. Computational Materials Science, 2018, 142, 59-71.	3.0	21
112	Dynamic interaction between grain boundary and stacking fault tetrahedron. Scripta Materialia, 2018, 144, 78-83.	5.2	41
113	A dual fracture transition mechanism in nanotwinned Ni. Materials Letters, 2018, 210, 243-247.	2.6	1
114	Self-accelerating sulfur reduction via polysulfide to realize a high-rate sulfidogenic reactor for wastewater treatment. Water Research, 2018, 130, 161-167.	11.3	69
115	Goal-Oriented Regional Angular Adaptive Algorithm for the <i>S_N</i> Equations. Nuclear Science and Engineering, 2018, 189, 120-134.	1.1	16
116	Elemental sulfur as an electron acceptor for organic matter removal in a new high-rate anaerobic biological wastewater treatment process. Chemical Engineering Journal, 2018, 331, 16-22.	12.7	39
117	Analysis of Spatial Discretization Error Estimators Implemented in ARES Transport Code for <mml:math <br="" xmlns:mml="http://www.w3.org/1998/Math/MathML">id="M1"><mml:mrow><mml:msub><mml:mrow><mml:mi mathvariant="normal">S</mml:mi </mml:mrow><mml:mrow><mml:mi>N</mml:mi></mml:mrow></mml:msub></mml:mrow></mml:math>	0.8 • <td>1 row> </td>	1 row>
118	Equations. Science and Technology of Nuclear Installations, 2016, 2016, 1-10. Interethnic analyses of blood pressure loci in populations of East Asian and European descent. Nature Communications, 2018, 9, 5052.	12.8	75
119	Nonlinear elastic response of single crystal Cu under uniaxial loading by molecular dynamics study. Materials Letters, 2018, 227, 236-239.	2.6	24
120	New insights into the effects of support matrix on the removal of organic micro-pollutants and the microbial community in constructed wetlands. Environmental Pollution, 2018, 240, 699-708.	7.5	31
121	3-D Drone-Base-Station Placement With In-Band Full-Duplex Communications. IEEE Communications Letters, 2018, 22, 1902-1905.	4.1	49
122	Regression models with ordered multiple categorical predictors. Journal of Statistical Computation and Simulation, 2018, 88, 3164-3178.	1.2	4
123	Atomistic Simulation of the Interaction Between Point Defects and Twin Boundary. Physica Status Solidi (B): Basic Research, 2018, 255, 1800228.	1.5	3
124	Geological and isotopic constraints on ore genesis, Huangjindong gold deposit, Jiangnan Orogen, southern China. Ore Geology Reviews, 2018, 99, 264-281.	2.7	33
125	Ibuprofen and iohexol removal in saturated constructed wetland mesocosms. Ecological Engineering, 2017, 98, 394-402.	3.6	48
126	All-Fiber Generation of Sub-30 fs Pulses at 1.3-μm via Cherenkov Radiation With Entire Dispersion Management. Journal of Lightwave Technology, 2017, 35, 2325-2330.	4.6	14

#	Article	IF	CITATIONS
127	The formation and destruction of stacking fault tetrahedron in fcc metals: A molecular dynamics study. Scripta Materialia, 2017, 136, 78-82.	5.2	38
128	Functionality of microbial communities in constructed wetlands used for pesticide remediation: Influence of system design and sampling strategy. Water Research, 2017, 110, 241-251.	11.3	82
129	Deformation mechanisms in nanotwinned copper by molecular dynamics simulation. Materials Science & Engineering A: Structural Materials: Properties, Microstructure and Processing, 2017, 687, 343-351.	5.6	51
130	A high-rate sulfidogenic process based on elemental sulfur reduction: Cost-effectiveness evaluation and microbial community analysis. Biochemical Engineering Journal, 2017, 128, 26-32.	3.6	27
131	Effects of constructed wetland design on ibuprofen removal – A mesocosm scale study. Science of the Total Environment, 2017, 609, 38-45.	8.0	64
132	Calculation of the C5G7 3-D extension benchmark by ARES transport code. Nuclear Engineering and Design, 2017, 318, 231-238.	1.7	8
133	High-Speed Random Bit Generation via Brillouin Random Fiber Laser With Non-Uniform Fibers. IEEE Photonics Technology Letters, 2017, 29, 1352-1355.	2.5	13
134	Influence of temperature and local structure on the shear-coupled grain boundary migration. Physica Status Solidi (B): Basic Research, 2017, 254, 1600477.	1.5	17
135	Stacking fault tetrahedron induced plasticity in copper single crystal. Materials Science & Engineering A: Structural Materials: Properties, Microstructure and Processing, 2017, 680, 27-38.	5.6	41
136	Thermochronologic constrains on the processes of formation and exhumation of the Xinli orogenic gold deposit, Jiaodong Peninsula, eastern China. Ore Geology Reviews, 2017, 81, 140-153.	2.7	42
137	Microbial community metabolic function in constructed wetland mesocosms treating the pesticides imazalil and tebuconazole. Ecological Engineering, 2017, 98, 378-387.	3.6	32
138	Evaluation of Mechanical Properties of Σ5(210)/[001] Tilt Grain Boundary with Self-Interstitial Atoms by Molecular Dynamics Simulation. Journal of Nanomaterials, 2017, 2017, 1-11.	2.7	6
139	ARES: A Parallel Discrete Ordinates Transport Code for Radiation Shielding Applications and Reactor Physics Analysis. Science and Technology of Nuclear Installations, 2017, 2017, 1-11.	0.8	17
140	Experimental Study on Variation Rules of Damping with Influential Factors of Tuned Liquid Column Damper. Shock and Vibration, 2017, 2017, 1-17.	0.6	1
141	Analyses of the TIARA 43 MeV Proton Benchmark Shielding Experiments Using the ARES Transport Code. Science and Technology of Nuclear Installations, 2017, 2017, 1-5.	0.8	Ο
142	The effect of an orifice plate with different orifice numbers and shapes on the damping characteristics of a dual-chamber air spring. Journal of Vibroengineering, 2017, 19, 2375-2389.	1.0	3
143	Evaluation of PWR pressure vessel fast neutron fluence benchmarks from NUREC/CR-6115 with ares transport code. Nuclear Technology and Radiation Protection, 2017, 32, 204-210.	0.8	5
144	The Stiffness and Damping Characteristics of a Dual-Chamber Air Spring Device Applied to Motion Suppression of Marine Structures. Applied Sciences (Switzerland), 2016, 6, 74.	2.5	15

#	Article	IF	CITATIONS
145	Indirect sulfur reduction via polysulfide contributes to serious odor problem in a sewer receiving nitrate dosage. Water Research, 2016, 100, 421-428.	11.3	71
146	Strengthening mechanisms and dislocation processes in <111> textured nanotwinned copper. Materials Science & Engineering A: Structural Materials: Properties, Microstructure and Processing, 2016, 676, 474-486.	5.6	20
147	Anycast Planning in Space Division Multiplexing Elastic Optical Networks With Multi-Core Fibers. IEEE Communications Letters, 2016, 20, 1983-1986.	4.1	40
148	Coupled grain boundary motion in aluminium: the effect of structural multiplicity. Scientific Reports, 2016, 6, 25427.	3.3	29
149	Effects of Lead and Mercury on Sulfate-Reducing Bacterial Activity in a Biological Process for Flue Gas Desulfurization Wastewater Treatment. Scientific Reports, 2016, 6, 30455.	3.3	43
150	Removal of the pesticides imazalil and tebuconazole in saturated constructed wetland mesocosms. Water Research, 2016, 91, 126-136.	11.3	70
151	Plasma Metabonomic Profiling of Diabetic Retinopathy. Diabetes, 2016, 65, 1099-1108.	0.6	113
152	A review on atomistic simulation of grain boundary behaviors in face-centered cubic metals. Computational Materials Science, 2016, 118, 180-191.	3.0	78
153	A dual deformation mechanism of grain boundary at different stress stages. Materials Letters, 2016, 167, 278-283.	2.6	9
154	Thermochronologic constraints on evolution of the Linglong Metamorphic Core Complex and implications for gold mineralization: A case study from the Xiadian gold deposit, Jiaodong Peninsula, eastern China. Ore Geology Reviews, 2016, 72, 165-178.	2.7	93
155	The shear response of copper bicrystals with $\hat{L}11$ symmetric and asymmetric tilt grain boundaries by molecular dynamics simulation. Nanoscale, 2015, 7, 7224-7233.	5.6	50
156	Verification of ARES transport code system with TAKEDA benchmarks. Nuclear Instruments and Methods in Physics Research, Section A: Accelerators, Spectrometers, Detectors and Associated Equipment, 2015, 797, 297-303.	1.6	8
157	Axial and Transverse Coupled Vibration Characteristics of Deep-water Riser with Internal Flow. Procedia Engineering, 2015, 126, 260-264.	1.2	10
158	Brittle versus ductile behaviour of nanotwinned copper: A molecular dynamics study. Acta Materialia, 2015, 89, 1-13.	7.9	42
159	Numerical simulation of bubble dynamics and heat transfer with transient thermal response of solid wall during pool boiling of FC-72. International Journal of Heat and Mass Transfer, 2015, 84, 409-418.	4.8	27
160	Ductile-to-brittle fracture transition in polycrystalline nickel under tensile hydrostatic stress. Computational Materials Science, 2015, 109, 147-156.	3.0	8
161	A New Energy-Absorbing Device for Motion Suppression in Deep-Sea Floating Platforms. Energies, 2015, 8, 111-132.	3.1	19
162	Brittle versus ductile fracture behaviour in nanotwinned FCC crystals. Materials Letters, 2015, 152, 65-67.	2.6	13

#	Article	IF	CITATIONS
163	Molecular dynamics study on the grain boundary dislocation source in nanocrystalline copper under tensile loading. Materials Research Express, 2015, 2, 035009.	1.6	26
164	Highly efficient data migration and backup for big data applications in elastic optical inter-data-center networks. IEEE Network, 2015, 29, 36-42.	6.9	324
165	Global Metabonomic and Proteomic Analysis of Human Conjunctival Epithelial Cells (IOBA-NHC) in Response to Hyperosmotic Stress. Journal of Proteome Research, 2015, 14, 3982-3995.	3.7	25
166	Influence of heater thermal capacity on bubble dynamics and heat transfer in nucleate pool boiling. Applied Thermal Engineering, 2015, 88, 118-126.	6.0	34
167	Fluid immiscibility and gold deposition in the Xincheng deposit, Jiaodong Peninsula, China: A fluid inclusion study. Ore Geology Reviews, 2015, 65, 701-717.	2.7	85
168	Influence of Transient Thermal Response of Solid Wall on Bubble Dynamics in Pool Boiling. Journal of Computational Multiphase Flows, 2014, 6, 313-327.	0.8	4
169	Influence of Transient Thermal Response of Solid Wall on Bubble Dynamics in Pool Boiling. Journal of Computational Multiphase Flows, 2014, 6, 361-375.	0.8	1
170	Spectrum-efficient anycast in elastic optical inter-datacenter networks. Optical Switching and Networking, 2014, 14, 250-259.	2.0	43
171	Atomistic Simulation of Tensile Deformation Behavior of â^5 Tilt Grain Boundaries in Copper Bicrystal. Scientific Reports, 2014, 4, 5919.	3.3	59
172	A novel approach to realize SANI process in freshwater sewage treatment – Use of wet flue gas desulfurization waste streams as sulfur source. Water Research, 2013, 47, 5773-5782.	11.3	80
173	Dynamic Service Provisioning in Elastic Optical Networks With Hybrid Single-/Multi-Path Routing. Journal of Lightwave Technology, 2013, 31, 15-22.	4.6	424
174	Energy-Efficient Translucent Optical Transport Networks With Mixed Regenerator Placement. Journal of Lightwave Technology, 2012, 30, 3147-3156.	4.6	42
175	Topological structure evolvement of flow and temperature fields in deformable drop Marangoni migration in microgravity. International Journal of Heat and Mass Transfer, 2011, 54, 4655-4663.	4.8	25